

Towards Realistic Statistical Models of the Grid Frequency

David Kraljic

Abstract—Increased share of renewable sources of energy in a power grid leads to larger deviations in grid frequency from the nominal value resulting in more challenging control and its modelling. In this paper we focus on the grid frequency for the power system of Great Britain because the large share of renewables makes it a template for other power grids in the future and because it exhibits peculiar statistical properties, such as long-term correlations in fluctuations, periodicity, bi-modality, and heavy tails in the distribution of the grid frequency. By modifications of the swing equation and the underlying noise statistics, which we justify qualitatively and quantitatively, we reproduce these peculiar statistical properties. We apply our model to realistic frequency response services and show our predictions outperform a standard swing equation model.

Index Terms—Stochastic processes, Power system modeling, Frequency, Power system simulation

I. INTRODUCTION

The integration of renewable sources of energy into power grids is an ongoing trend which is mostly driven by an attempt to reduce the emissions of green-house gases during electricity production. The most prominent renewable sources are wind and solar power which are by their nature fluctuating and uncontrollable. High wind and solar share of power generation are typically associated with low effective inertia of the grid which leads to challenges in integrating them into a power system. Power grid with a significant share of renewables is susceptible to larger deviations in the grid frequency [1], [2] which leads to increase in procurement of reserve and ancillary services aimed at stabilising the grid. In recent years, due to the increased share of renewables, the typical size of deviations has been increasing [1], thereby increasing the probability of outages.

Realistic and detailed models of the grid frequency are therefore needed for future-proofing the grid. Modelling of the grid frequency underlies, for example, the estimation of the size of reserve and frequency response services that need to be procured as well as the estimation of the usage of assets, income, and risk of providers of such services.

Most models for the grid frequency start with the swing equation [3]. In order to include fluctuations inherent in the power system, the equation is upgraded to a stochastic differential equation resulting in a form of Ornstein-Uhlenbeck Process (OUP) [4]. The simplest models add a stochastic term directly to the swing equation and assume that fluctuations are adequately described by Gaussian noise [5]–[7]. Another approach, following [4], is to model the load fluctuations in

the swing equation as an OUP (empirically supported by [8]), leading to two stochastic equations, one for the load and one for the grid frequency, resulting in a Brownian stochastic term for the swing equation [9], [10]. As we will see in later sections, the properties of the ‘random’ process underpinning the fluctuation in grid frequency exhibit a wealth of structure beyond Gaussian or Brownian.

Statistical modelling of grid frequency in literature usually focuses on the *aggregated* values such as the probability density function (PDF). Some approaches study frequency as a *timeseries*, which focuses on quantities such as the auto-correlation function (ACF). However, there has been little work on models that reproduce both the timeseries and aggregated properties.

The most salient feature of the grid frequency timeseries, the periodicity in the fluctuations, was identified to be caused by trading on the market [11]. Reference [12] attempts to model these periodic effects, which show in the ACF, by the deterministic and periodic imbalance generated by the market while using Gaussian noise for the stochastic part. This reproduced the initial exponential drop-off of the ACF and the periodic peaks but had a mismatch in the tails and at the centre of the PDF for the grid frequency. Reference [13] shows that the tails of the PDF for the grid frequency in continental Europe are heavier than Gaussian and finds that sourcing the noise from Lévy stable distributions improves the fit in the PDF tails, but now over-estimates the tails. Reference [14] improves on the goodness of fit of the PDF by solving the swing equation with Gaussian noise that has the mean and variance changing slowly with time, leading to q-Gaussian final distributions. Reference [15] combines this noise model with the insight that the periodicity of the electricity market is responsible for the periodicity of the ACF leading to good quantitative fits to the PDF in the tails and rough qualitative agreement for the ACF.

Grid frequency PDFs for different synchronous areas can roughly be separated in single-peaked and multi-peaked distributions [16]. Reference [10] has used the stochastic formulation of [4] and identified the governor deadband as the main ingredient for successfully reproducing the double-peakedness of the frequency PDF for Great Britain. Similarly, detailed modelling of various frequency controllers identified the deadband as the primary reason for double-peakedness of the Irish grid [9]. Reference [17] has further investigated the parameters in the swing equation (with an additional load OUP) to show that double-peakedness can be robustly removed with synthetic inertia.

In contrast to statistical modelling of the grid frequency, one

D. Kraljic is with Faculty of Electrical Engineering, University of Ljubljana, Ljubljana, Slovenia and with Comcom Trading d.o.o., Slovenia

can attempt to predict it for some time frame in the future. Reference [18] uses predictive models based on nearest-neighbour techniques, whereas [19] uses auto-regressive models. To avoid purely statistical analysis some properties of the grid frequency fluctuations can be explained by physical reasons. For example, [20] finds that wind profiles and particular locations of power injection exacerbate the non-Gaussianity of frequency fluctuations.

We select the power system of Great Britain (GB) for studying the statistical properties of grid frequency fluctuations. The GB system is its own synchronous area, so it can be studied in isolation. It is small (compared to e.g. the European Continental Synchronous Area), leading to low inertia, and has a large share of renewable energy¹. Therefore, it can be considered as a template for future grids elsewhere. Another reason for selecting the GB grid frequency is the fact that it exhibits non-trivial properties both in ACF *and* PDF. Therefore, the methods in this paper that successfully model both can be extended to other synchronous areas with similar or simpler statistical properties. In the Appendix we show that similar statistical properties hold for several other synchronous grids.

In Section II we present the statistical properties of the grid frequency we aim to reproduce with our modelling. In Section III we present the physical basis for the modelling, whereas in Section IV we present a phenomenological model derived from the physical model. In Section V we describe the data used in the analyses. In Section VI we show the results, discuss them, and use them in a real-world application.

A. Our contribution

The overall contribution of the paper is a stochastic model of the grid frequency that reproduces the long-range dependence of fluctuations *and* bi-modality of the distribution *and* the heavy-tails of the distribution. All of these properties have not been captured so far in a single model and we achieve it with the same number of parameters as comparable models in literature. In detail:

- 1) We show that the ACF has a power-law behaviour and we successfully model it with fractional noise. We show that the power-law cannot be reproduced by the usual non-fractional Gaussian or Lévy type noise within a swing equation framework.
- 2) We show that the PDF has heavy tails and we successfully model it with noise that is both fractional and heavy-tailed (Lévy stable)
- 3) We empirically show that the effective damping factor (related to inertia and droop) is dependent on the grid frequency and describe a method of obtaining the values from the data.
- 4) We model yearly energy and time requirements for two types of reserve services and show that our model outperforms the models based on Gaussian noise.

II. THE STATISTICAL PROPERTIES OF THE GB GRID FREQUENCY

In this section we present the most salient statistical properties of the real GB grid frequency which we aim to reproduce in our models. The detailed discussion and modelling are deferred to later sections. The grid frequency fluctuates around its central value of 50 Hz, so naively we would expect the most likely value to be 50 Hz. However, the PDF of GB grid frequency (and many other grids) exhibits two peaks (Fig. 1), meaning that frequency spends more time slightly above or below the central value. The next property of the PDF reveals itself on its log-log plot (Fig. 5) where we see that the tails of the distribution are heavier than what would be expected from Gaussian fluctuations. Usually, Gaussian fluctuations are expected as they arise via the Central Limit Theorem when many different fluctuating contributions sum up (e.g. in a power system). Heavy tails mean that the real grid frequency often exhibits large deviations.

Deviation of the grid frequency away from the central value is not independent from one time instant to another, because the fluctuations driving the grid frequency, i.e. the noise, are adding up over time. The dependence over time is captured by the ACF (Fig. 2). We would like to capture both the short term drop-off, that measures how strongly the value of grid frequency is pushed towards the center, and the long-term power-like tail, that signals that deviations away from the central value can persist for hours. We would also like to mimic the periodic nature in the ACF (Fig. 3). Summarized properties that our model aims to capture are:

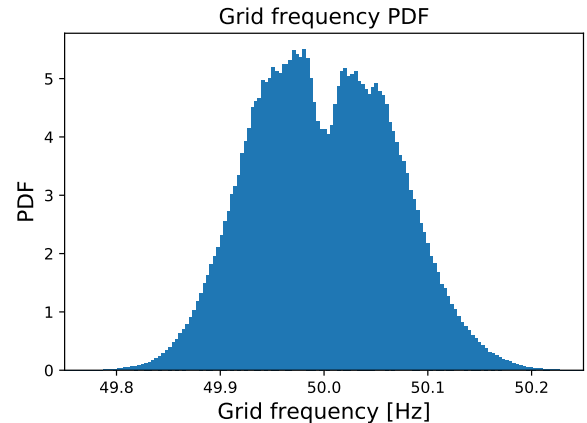


Fig. 1. Histogram (PDF) of the GB grid frequency. Note the bi-modal (double-peaked) structure.

- 1) The grid frequency PDF
 - a) The bi-modal (double-peaked) structure, Fig. 1
 - b) The overall scale of fluctuations
 - c) The heavy tails, Fig. 5
- 2) The autocorrelation function / phase dispersion periodogram
 - a) The exponential drop for short lags ($\lesssim 10$ min), Fig. 2
 - b) The periodicity of signal, Figs. 2, 3

¹See e.g. <https://www.iea.org/data-and-statistics>

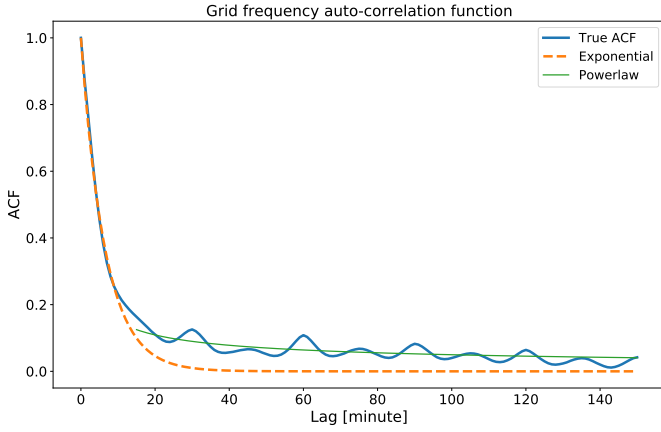


Fig. 2. Autocorrelation of the GB grid frequency with lags up to 2.5 hours (150 minutes). Note the quick exponential decay initially followed by a slow power-law-like decrease later.

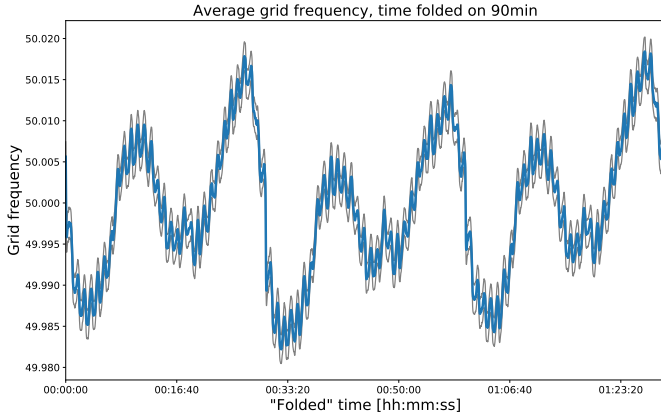


Fig. 3. Phase dispersion periodogram – average grid frequency with time ‘folded’ on the period of 90 minutes. This means that, for example, the value for the time label 00:00:12 is the average of grid frequency at times 00:00:12, 01:30:12, 03:00:12, etc.. The two standard deviation bands are plotted in grey.

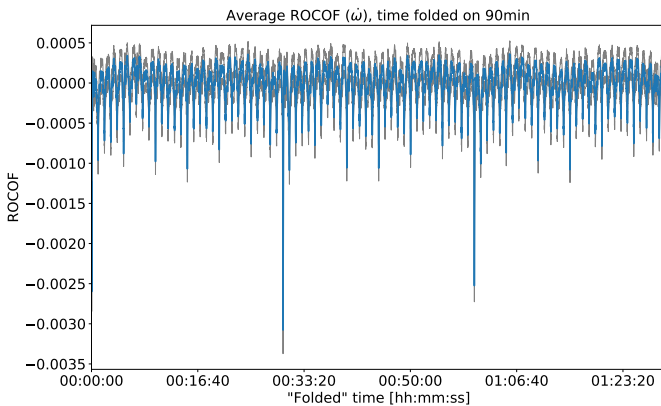


Fig. 4. Phase dispersion periodogram – average ROCOF (rate of change of frequency), time ‘folded’ on the period of 90 minutes. The two standard deviation bands are plotted in grey.

- c) The second-by-second structure (within timescale of exponential drop), Figs. 3, 4
- d) The power-law like long range correlation, Fig. 2

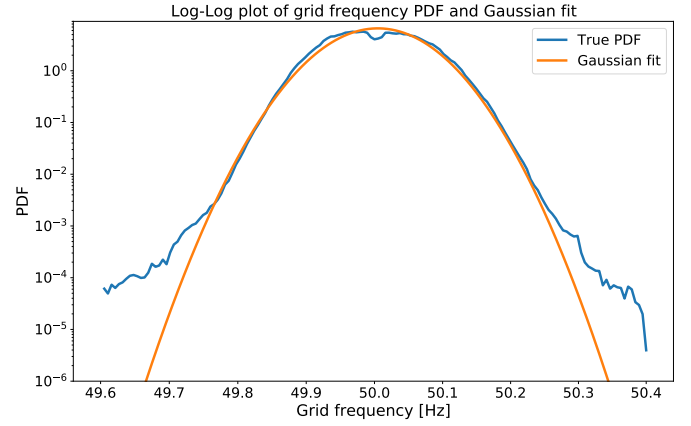


Fig. 5. Log-Log plot of the PDF, with best-fit Gaussian overlaid. Note that the PDF above ± 0.2 Hz exhibits heavier tails than Gaussian.

III. THE PHYSICAL BASIS FOR THE MODEL

The electric grid consists of many interconnected generators and consumers of power, each of which can be considered as an oscillator producing/consuming power at the frequency close to the nominal grid frequency Ω (e.g. 50 Hz). The following analysis closely follows [21]. The phase angle at a generator i is:

$$\theta_i = \Omega t + \tilde{\theta}_i \quad (1)$$

where $\tilde{\theta}_i$ is the small phase perturbation relative to the whole grid. The power of the generator is then:

$$P_i = P_i^{\text{dissipated}} + P_i^{\text{accumulated}} + P_i^{\text{transmitted}} \quad (2)$$

where the dissipated power is due to friction, the accumulated power is stored in rotational kinetic energy, and the transmitted power is due to the phase difference between this generator and the rest of them:

$$P_i^{\text{dissipated}} \propto (\dot{\theta}_i)^2, \quad (3)$$

$$P_i^{\text{accumulated}} \propto M_i \frac{d}{dt} (\dot{\theta}_i)^2, \quad (4)$$

$$P_i^{\text{transmitted}} \propto \sum_{j \neq i} K_{i,j} \sin(\theta_j - \theta_i), \quad (5)$$

where M_i is the generator moment of inertia, $K_{i,j}$ contains the information on the topology and transmission capacity of the grid (which generators are connected and the amplitude of the power flow between them), and is symmetric in indices.

Expanding each term on the right-hand-side of (2) to first order in perturbations $\tilde{\theta}_i$ and dividing everything by the moment of inertia M_i results in:

$$\ddot{\tilde{\theta}}_i = p_i - \alpha_i \dot{\tilde{\theta}}_i + \sum_{j \neq i} k_{i,j} \sin(\theta_j - \theta_i) \quad (6)$$

where parameter $p_i = P_i/M_i$ corresponds to the power of generator i , α_i to the magnitude of friction, and $k_{i,j} = K_{i,j}/M_i$ to the amount of power that can be transmitted between generator i and j .

The overall grid frequency ω is the nominal value Ω plus the sum (weighted by the inertia of each generator) of all individual perturbations:

$$\omega = \Omega + \sum_i M_i \tilde{\theta}_i / \sum_i M_i \quad (7)$$

which results in the ‘swing equation’:

$$\dot{\omega} = -\gamma\omega + \pi(t) \quad (8)$$

where the first restoring term on the right-hand-side contains is pulling the grid frequency towards the nominal value Ω (which we dropped for convenience and without loss of generality) and the second term $\pi(t)$, which perturbs the grid frequency, contains the sum of all generated and consumed powers at each generator:

$$\pi(t) \propto \sum_i M_i P_i \quad (9)$$

The swing equation (8) is of the form as in e.g. [9], [14]. There is an equivalent formulation, as in e.g. [4], [10]:

$$2H\dot{\omega} = -\alpha\omega + \pi(t), \quad (10)$$

where H is the aggregated inertia constant and α is the inverse aggregated droop coefficient. Note that if we increase or decrease the inertia H , droop α , and the size of the noise term $\pi(t)$ by the same factor, the dynamics of grid frequency as described by the swing equation does not change. Therefore, when simulating the swing equation, there is a degeneracy among these parameters. However, we can constrain the ratios, e.g. $\gamma = \alpha/2H$, so we choose the swing equation parametrization as in (8).²

IV. THE PHENOMENOLOGICAL MODEL

The physical model of (8) forms the basis of our modelling of the grid frequency. The physical model contains two unknowns – the perturbation term $\pi(t)$ and the decay factor γ . In this section we consider what determines the values and structure of these unknowns and how they can be empirically modelled.

A. The nature of perturbation term $\pi(t)$

In [14] it is assumed that the powers sum to zero and all that remains is unstructured noise (either of Gaussian or Lévy type) of unknown origin or cause. Specifically, it is assumed that the noise at two different times is uncorrelated. In reality, the powers do not sum to zero at each time instant, as the residual is what drives grid frequency away from the nominal value, and the term $\pi(t)$ contains a wealth of stochastic and deterministic structure. Of course, the residual of the sum of powers of all rotors can be in first instance approximated as a noise term.

²Inertia constant and droop can be estimated if the parameter degeneracy is broken by a known size of the power fluctuation $\pi(t)$, e.g. during the first few seconds of a sudden outage of a large power plant.

a) *Random part:* The random part of $\pi(t)$ is caused, for example, by the variability in production of renewable generation, the forecast error in demand, the forecast error of the market regarding imbalance, as well as the effect of faults in the grid (generator tripping). The information on the forecast errors is not available immediately, the error is not rectified immediately (e.g. weather forecast run only a few times daily), and the information does not spread efficiently to all the active participants in the grid (generators, electricity system operators (ESO), traders). This means that the random part of the frequency deviation might exhibit long term dependence.

b) *Non-random part:* The non-random part of $\pi(t)$ is influenced, for example, by the scheduled decisions of generators, the balancing actions of the ESO, the developments on the power market, the automatic activation of reserve services, generators speculating on the imbalance price, and generators misreporting their physical position. All of the listed things are tied to the common structure – the settlement of imbalances, which is performed at half-hourly intervals in GB, and the market contracts that are structured into half-hourly, 1-hour, 2-hour, and 4-hour blocks. Therefore, we expect deterministic structure to appear and be periodic at these time scales.

The non-random part of $\pi(t)$ also contains responses to the system imbalances by active participants in the grid, which can all be described as terms of the restoring form like $-\gamma^{\text{parti}}\omega$. For example, the ESO is actively pursuing the balance of the electric system, so its actions can be described by a restoring term. The market, through matching the supply and demand, is also driving the system towards balance and can be described by a restoring term. The reserve (a.k.a frequency response) triggered at certain deviations from the nominal frequency and proportional to the size of deviation can be faithfully modelled by a restoring term. Imbalance speculating generators that intentionally produce imbalance to collect payment according to the imbalance price also drive the system towards stability, and consequently frequency towards the nominal value.

Therefore, after removing the terms of the restoring form, the non-random part of the noise term in (8) can be decomposed into the pure noise term $\xi(t)$ (of unit variance) with the mean $\mu(t)$ and variance $\sigma(t)$ being periodic functions determined by e.g. the periodicity of the market (as in Fig. 3):

$$\pi(t) = \mu(t) + \sigma(t) \cdot \xi(t) \quad (11)$$

B. The nature of damping factor γ

The restoring term $-\gamma(\omega - \Omega)$ in (8) is in part physical in origin and is determined by the moment of inertia and droop of all the generators in the grid (10).

In most studies so far the damping factor γ has been assumed to be constant in time, with the exception of [14]. In fact, due to the varying share of renewable generation in the grid, the moment of inertia of the grid is lower during times of high share of renewable generation. For a review, see [22], [23]. Therefore, we expect γ to be a slowly (compared to $\pi(t)$) varying function of time.

The restoring part of (8) has multiple contributions in addition to the physical in origin. As discussed in Sec. IV-A,

TABLE I
TYPES OF NOISE AND THEIR PROPERTIES

Property	Gaussian / Lévy	Fract. Gaussian / Lévy
Mean $\langle \xi(t) \rangle$	0	0
Correlation $\langle \xi(t)\xi(t') \rangle$	$\propto \delta(t-t')$	$\propto t-t' ^{2H-2}$
Tails	normal / fat	normal / fat

the active participants in the grid (generators, ESO, traders, reserve services) also contribute terms of the restoring form. Therefore, the restoring term is described by the sum of all contributions as an overall effective damping factor γ^{eff} .

We expect the effective damping factor γ^{eff} to have a dependence on the value of grid frequency. The main physical reason are governor deadbands. Other restoring terms non-physical in origin also contain ‘deadbands’. For example, ESO does not react to the smallest system imbalance (as manifested in frequency deviation) and instructs power plants only when deviation is big enough. Additionally, reserve services are only triggered above/below a certain threshold. All of these effects combine into strong ω dependence of the effective damping term γ^{eff} :

$$\dot{\omega} = -\gamma^{eff}(t, \omega) \cdot \omega + \pi(t) \quad (12)$$

where $\pi(t)$ now contains only the random and periodic components (11). In this paper we will not focus on the time dependence of γ^{eff} but instead on the dependence on ω .

C. Modelling the noise $\xi(t)$

The restoring term of (8) is responsible for the initial exponential decay of the ACF. In the case where γ^{eff} is constant and $\pi(t)$ is uncorrelated Gaussian noise, the model is known as the Ornstein-Uhlenbeck [24] (or Vasicek [25]) model and has an autocorrelation function that decays exponentially with the decay factor γ^{eff} .

Extending such a model by heavy-tailed noise sourced from e.g. a Lévy stable distribution does not change the exponential drop of the ACF. This can be seen by integrating (8) and calculating the correlator $\langle \omega(t)\omega(t') \rangle$ [26]. We use the fact that for Gaussian and Lévy type noise $\langle \xi(t)\xi(t') \rangle \propto \delta(t-t')$, where $\delta(t-t')$ is the Dirac delta function. That is, the noise two-point correlation function is non-vanishing only when evaluated at the same instant [27]. Therefore, the long-range dependence seen empirically in the ACF (see Fig. 2) cannot be produced by these types of noise.

a) Long-range dependence via Fractional noise: Long term dependence, power-law behaviour, and long-term memory processes are frequently described using ‘fractional noise processes’ [28]–[30]. For example, Fractional Gaussian Noise is a generalisation of Gaussian noise for which the correlation of the noise term at two different time instants does not vanish and thus leads to long-range dependence in the ACF.

Long-range behaviour of fractional noises is characterised by a single parameter H , called the Hurst exponent. Uncorrelated behaviour is reproduced for $H = 1/2$, $1 > H > 1/2$ results in positive long-range autocorrelations, and $0 < H < 1/2$ results in short-term autocorrelations.

Heavy tails can also be modelled within the fractional noise framework, where the underlying noise is sourced from a Lévy stable distribution [31], thus achieving both the long-range correlations and large point-wise fluctuations. This type of noise is termed Fractional Lévy Noise (FLN) [32]. We are interested in noise distributions without skew. Therefore the Lévy stable distributions we consider are characterized by one parameter $\alpha \in (0, 2]$ which controls the fatness of tails, where values below 2 correspond to heavy tails.

Standard uncorrelated Gaussian noise leading to OUP swing equation, used in e.g. [9], [10], is reproduced for parameter combination $H = 1/2$ and $\alpha = 2$.

Fractional noise processes have found application in a variety of fields (e.g. economics [33], hydrology [34], engineering [35]...). The properties of different noise types are summarized in Table I.

V. THE DATA

The data on GB grid frequency was obtained from the electricity system operator (ESO) in Great Britain [36] and it consists measurements of the grid frequency floored to three decimal places with granularity of 1 second. We study the data from 2014 to 2020 inclusive.

VI. RESULTS AND DISCUSSION

A. Autocorrelation function: the exponential part

The autocorrelation function has an initial exponential decay and a long-range power-law like part (see Fig. 2). For lags $\lesssim 15$ min the ACF can then be modelled as $ACF(t) \sim \exp(-\gamma^{eff}t)$. The parameter γ^{eff} can be extracted by straight line fits on a semi-log plot of the ACF. The results of the fit is $\gamma^{eff} = (5.5 \pm 0.1 \text{ min})^{-1}$.

1) Dependence of γ^{eff} on ω : As explained in Sec.IV-B the effective damping factor is expected to have a dependence on the value of the grid frequency, i.e. $\gamma^{eff}(\omega)$.

To show this effect is present in the data we split the datasets in frequency bins (e.g. in bins of 0.1 Hz). Then we calculate the ACF for data falling in each of the bins and plot the results in Fig. 6. We plot the first few lag minutes in the ACF since the exponential drop-off there is controlled by γ^{eff} . We see that for frequencies closer to 50 Hz the fluctuations are correlated stronger and for longer time. This means that γ^{eff} is smaller closer to 50 Hz as was expected (Sec.IV-B). The values for $\gamma^{eff}(\omega)$ can finally be extracted as slopes to semi-log plot of Fig. 6.

B. Autocorrelation function: the power-law part

For the autocorrelations above roughly 15 min the behaviour of the ACF can be described as a power law, $ACF(t) \sim t^{-\alpha}$. The parameter α can be extracted by straight-line fits on the log-log plot of the ACF. The result of the fit is $\alpha = -0.5 \pm 0.1$.

We model long-range, power-law correlations, using fractional noise. The stochastic noise is described by one parameter, the Hurst exponent H , which leads to power-law ACF of t^{2H-2} [37], [38]. Grid frequency power-law fit leads to Hurst exponent of 0.75 ($2H - 2 = -0.5$), suggesting strong long-term dependence. An alternative approach to demonstrate short

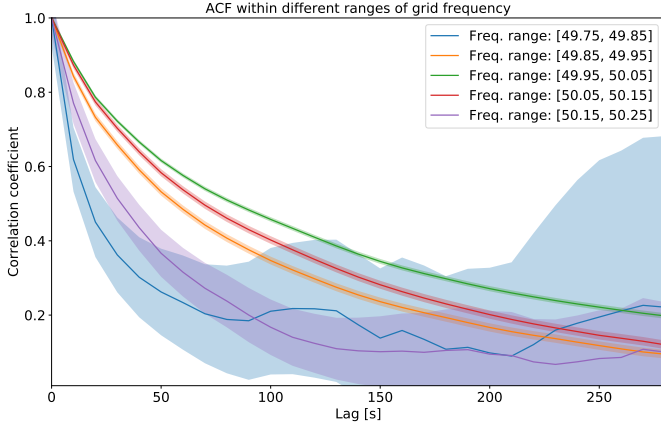


Fig. 6. ACF dependence on the grid frequency, in the regime where exponential drop-off is a good description. Note that when frequency is closer to 50 Hz we have stronger auto-correlations caused by lower γ^{eff} . Note that the error in ACF increases with lag distance (as there are fewer independent data points to estimate the ACF) and increases for bins far away from the nominal value, as the number of data points in those bins is small.

time exponential decay in the ACF and long time power law is by studying the power spectral density of the process, which we plot in Fig. 7. Power spectral density for the swing (OU, Vasicek) type of equation as (8) is described by the following expression [26]:

$$PSD(k) \sim \frac{\langle \tilde{\pi} \tilde{\pi}^* \rangle}{\gamma^2 + k^2} \quad (13)$$

where k is the inverse of the time scale, γ is the decay constant, and $\langle \tilde{\pi} \tilde{\pi}^* \rangle$ is the noise power spectrum. For Gaussian/Lévy noise this is just a constant (Fourier transform of the delta function). However, for fractional noise this term scales as $\langle \tilde{\pi} \tilde{\pi}^* \rangle \sim k^{-2H+1}$ [30], [38]. From the slope (-0.55 ± 0.04) at long times (small k) we show, that the underlying noise process is not Gaussian (slope should be 0) and obtain the Hurst exponent of about 0.75, consistent with estimation from the ACF.

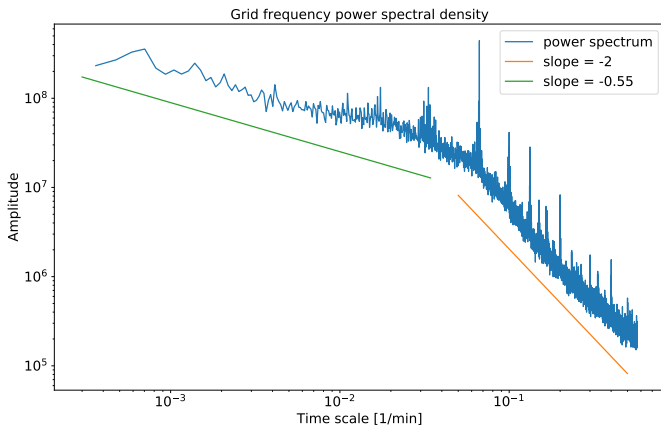


Fig. 7. Power spectral density of the grid frequency stochastic process. Note the Brownian/Gaussian scaling (slope=-2) at short times and fractional Brownian scaling at long times. For purely Gaussian noise the spectral density slope should be 0 at long times. Note the peaks due to periodicity.

TABLE II
MODEL PARAMETERS

Parameter	Value
Hurst exponent H	0.75
Lévy α	1.975
ω_{db}	15 mHz
γ_1	0
γ_2	1/150
σ	0.0021
$\mu(t)$	as in Fig.4

C. Probability density function: heavy tails

We generate heavy-tailed long-range Fractional Lévy Noise using our own efficient implementation³ of [39]. Parameter α that controls the fatness of tails can be in principle estimated from the data by e.g. a Hill estimator [40]. However, the grid frequency PDF is close to Gaussian (deviations away from Gaussian only above ± 0.2 Hz) suggesting that α is close to 2 (Gaussian case). In this parameter region estimators are unreliable [31]. Therefore, we perform a direct search via parameter sweep to find $\alpha = 1.975$ that best matches the tails of the GB grid frequency PDF (see Fig.10).

D. Simulation results

Equations (8) and (12) are stochastic differential equations, corresponding to a mean-reverting process. Numerical solutions to (8) and (12) are obtained using the Euler–Maruyama method [41]. The equations are solved using NUMPY software package [42].

We compare three models: a simple model based on the swing equation (8) with non-fractional Gaussian noise covers the majority of previous modelling attempts (see Section I), a detailed existing model for the GB grid frequency [10], and our model based on (12) with fractional Lévy noise for $\xi(t)$ and ω dependent γ^{eff} . The periodic component of the noise term $\mu(t)$ and scale of fluctuations σ are both taken from actual data which is summarised in Fig. 4. We model γ^{eff} with three parameters (as in e.g. [9], [10]):

$$\gamma^{eff}(\omega) \cdot \omega = \begin{cases} \gamma_1 \omega & -\omega_{db} \leq \omega \leq \omega_{db} \\ \gamma_2 \omega + (\gamma_2 - \gamma_1) \omega_{db} & \omega \leq -\omega_{db} \\ \gamma_2 \omega + (\gamma_1 - \gamma_2) \omega_{db} & \omega \geq \omega_{db} \end{cases} \quad (14)$$

where ω_{db} is the deadband frequency range and γ_1 is the damping term within the deadband and γ_2 outside of deadband.

With our model we can reproduce both the exponential drop-off and power-law tail in the ACF, as well as periodic structure (see Fig. 8). We can also reproduce the over-all scale of fluctuations and the double-peaked structure (Fig. 9). Moreover, our model also reproduces the heavy tails of the PDF (Fig. 10). This was achieved with the parameter combination in Table II.

Besides our model we reproduced the results of [10], labelled ‘Literature’. This particular model was selected to illustrate the importance of looking at all statistical properties

³https://github.com/davidkraljic/fractional_levy_motion

together. ‘Literature’ model agrees well with the PDF (Fig. 9) but does not capture the timeseries properties of the grid frequency at all (Fig. 8). For the class of simple baseline OU models with non-fractional Gaussian noise, labelled ‘Gaussian noise’ in the figures, we chose constant $\gamma^{eff}(\omega) = 1/400$ such that the initial exponential drop in the ACF is correctly captured and the overall scale $\sigma = 0.064$ of fluctuations is reproduced. Note that all models based on the swing equation and non-fractional Gaussian noise will fail to reproduce long-term correlations as seen in the ACF and the power spectrum even if the overall PDF and short term ACF fit well.

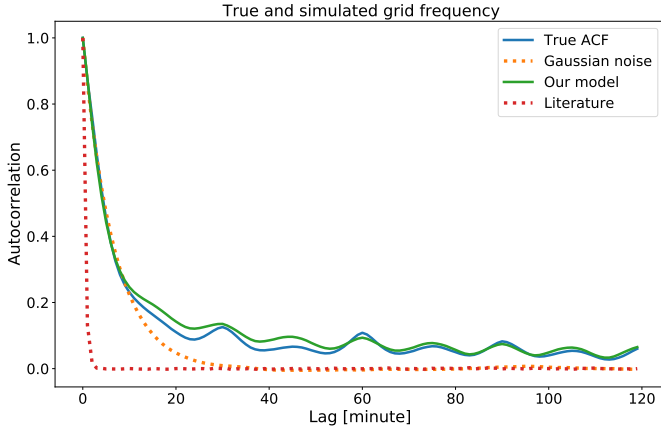


Fig. 8. True ACF compared with a simple OU model with Gaussian noise (model class as in [4], [6]–[9]), and our model based on (12) and Table II. A specific model from literature [10] is selected here to emphasise that while it matches the PDF well (Fig.9) it does not capture the time dynamics of grid frequency (encoded in ACF) at all.

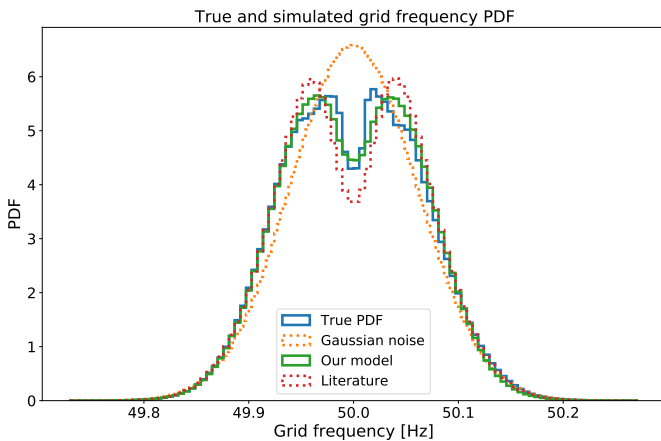


Fig. 9. True PDF compared with a simple OU model with Gaussian noise, and a model based on (12) and Table II, and a model from literature [10]. All models match the standard deviation and the mean of the actual frequency data.

E. Applications

More elaborate modelling of the grid frequency, compared with a simple OUP (i.e. non-fractional Gaussian noise), should lead to improvements in real-life applications of the models.

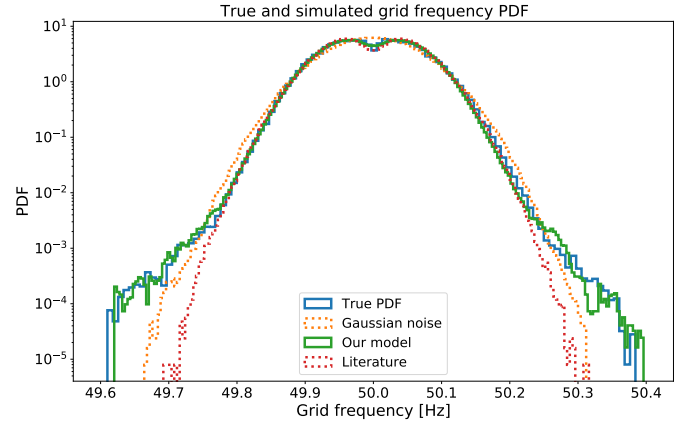


Fig. 10. Log plot of Fig.9 emphasising the tail behaviour.

Frequency response services are automatic balancing services provided by devices (batteries, diesel generators, industrial HVACs,...) to an ESO which are controlled by the value of the grid frequency. In general, in GB and elsewhere, there are two types of frequency response services: *dynamic*, where power generation/consumption of an asset is proportional to the deviation in the grid frequency after some trigger, and *static*, where power is generated/consumed at a fixed value after the service is triggered at some frequency deviation. If the devices delivering these services do not deliver the required energy for the required duration then strict financial penalties usually apply⁴.

a) Dynamic frequency response: Devices participating in the dynamic service (such as batteries) need to know the yearly distribution of energy requirements. The distribution is directly related to the timeseries of frequency fluctuations and is used to evaluate the ability of the device to deliver the service (or calculate the percentage of times the device will fail to deliver) as well as calculate the compensation for the provision of service as it is directly linked to the energy delivered.

We take the parameters for a typical GB high-frequency dynamic response service, where the proportional response is required within a couple of seconds for deviations above 50.015 Hz. In Fig.11 we plot the distribution of energy requirements for one year. We see that the Gaussian OUP, despite matching the over scale of fluctuations (see Figs.9, 8), underestimates larger energy requirements, due to the lack of long-term correlations in deviations from the nominal value, whereas our model reproduces the true requirement. This could lead to the wrong sizing of the battery destined for this service, wrong estimation of expected income, and higher than expected failure rate to delivery required energy. For example, looking at Fig. 11, using a simple OUP model to determine the size of a battery (determined by the largest energy requirement in a year) the owner of the device would size the battery to have capacity at 2000 (arb. units) but true requirement is closer to 3000 (arb. units).

b) Static frequency response: Similarly as above, evaluation of a device participating in a static delivery of frequency

⁴See <https://www.nationalgrideso.com/industry-information/balancing-services/frequency-response-services/firm-frequency-response-ffr>

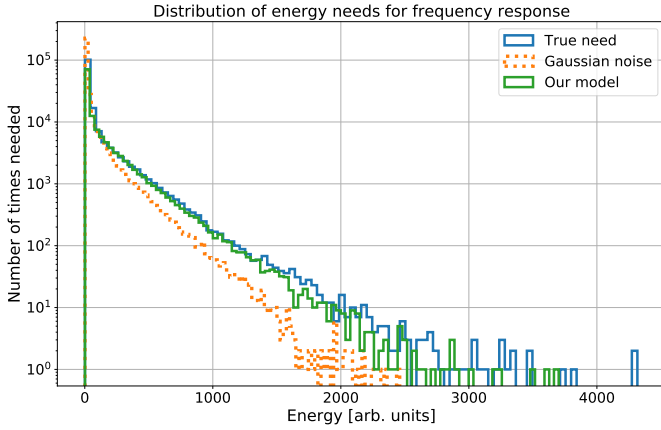


Fig. 11. Distribution of energy requirement in a year for a dynamic high frequency response as determined by our models vs true requirement and a model based on Gaussian noise.

response requires the knowledge of the distribution of response durations after each trigger. We take parameters for a typical low-frequency static response service, where a fixed power is generated within a couple of seconds for deviations below the 49.9Hz trigger. In Fig. 12 we plot the required response

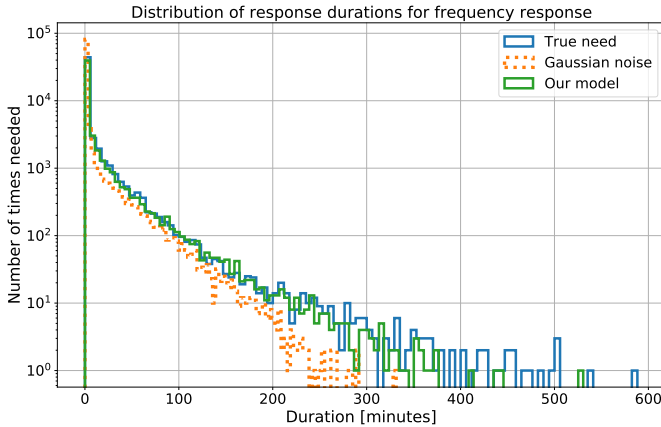


Fig. 12. Distribution of response durations in a year for a static low frequency response as determined by our models vs true requirement and a model based on Gaussian noise.

durations and again see that Gaussian OUP underestimates the frequency of the longer responses. For example, diesel generators that are committed to provide static response need to provide responses for the required length but are also limited to how long they can run in each year⁵ for environmental reasons. Using a simple OUP would underestimate the frequency of response durations (and consequently the amount of fuel needed) by more than a factor of two for events that would need responses longer than 2 hours (see Fig. 12).

c) Static frequency response and inertia change: Swing equation enables us, for example, the evaluation of what would requirement be for e.g. static frequency response if inertia in the grid changed with all other things being equal. Looking back at the derivation of the swing equation (8) and at the

form of the equation with explicit inertia constant (10) we see that lower inertia (while everything else stays the same) can be modelled by reducing the damping factor γ and size of fluctuations in $\pi(t)$ by the same factor. In Fig. 13 we compare two response duration distributions predicted by our model with differing inertia (by 20%). We see that lower

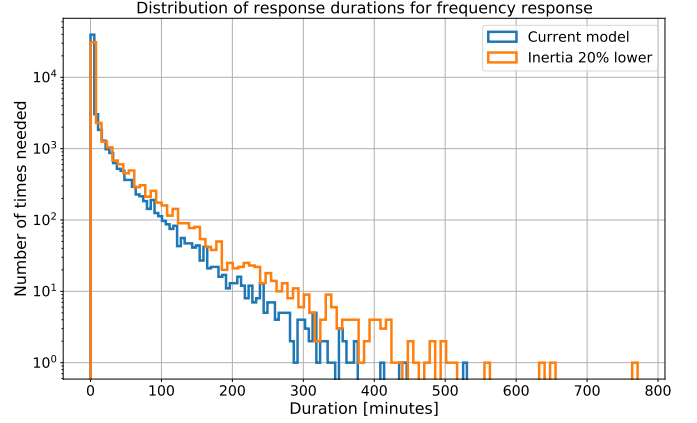


Fig. 13. Distribution of response durations in a year for a static low frequency response as determined by our model for differing grid inertia. Note that if the size of intrinsic fluctuations stays the same while the inertia decreases, the overall fluctuations in the grid frequency will increase (10). Because of long term correlations large deviations will persist for longer, requiring more frequent longer responses to frequency deviations.

inertia would mean more frequent long responses, as frequency deviations would stay longer below trigger level. For example, responses long about 2 hours would be twice as likely if overall yearly inertia would drop by 20% (all other things being equal).

VII. CONCLUSIONS

We study the statistical properties of the grid frequency, focusing on the data for the power system of Great Britain. We show that some curious statistical properties such as the double-peaked probability density function, heavy tails, periodicity, and the long-range power-law dependence in the autocorrelation function, can be modelled successfully by slight modifications of the swing equation or equivalently the Ornstein-Uhlenbeck stochastic process. We empirically show that the effective damping factor is frequency-dependent, which reproduces the double-peakedness. We show that a better description for the underlying noise process, compared to Gaussian, is fractional noise, which due to inherent long term correlations between noise increments reproduces the power-law behaviour in the autocorrelation function. Additionally, we source the fractional noise from heavy-tailed distribution to correctly capture the fat tails of the grid frequency probability density function. Finally, we look at applications of our model. We determine the distribution of energy requirement for a dynamic frequency response service, response duration distribution for a static frequency response service and show their predictions are closer to true values compared to predictions from a standard swing equation model.

⁵See e.g. <https://ec.europa.eu/environment/industry/stationary/mcp.htm>

VIII. ACKNOWLEDGMENTS

The author would like to thank the reviewers. Their suggestions have vastly improved the initial version of this contribution.

APPENDIX

STATISTICAL PROPERTIES OF OTHER GRIDS

A. European Continental Synchronous grid

We show that the European grid exhibits similar properties to the GB frequency: double-peakedness (Fig. 14), periodicity and long term correlations suggesting fractional noise fluctuations (Figs. 15, 16). Therefore same modelling approaches as in this paper can be used for the European grid. The data was obtained from the French ESO [43] and consists of measurements sampled every 10 seconds. We study the data from 2017 to 2020 inclusive.

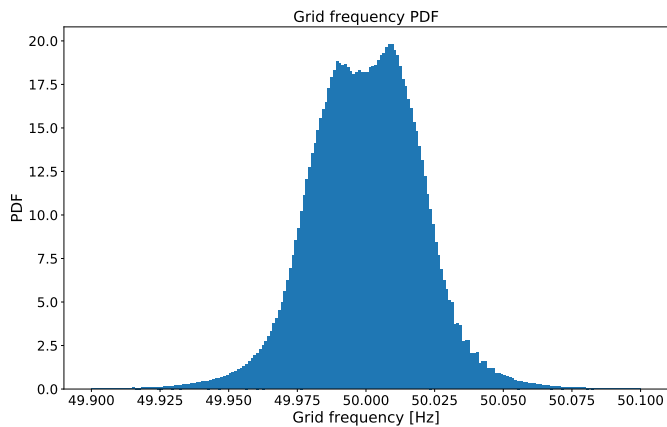


Fig. 14. European grid frequency PDF. Note the slight double-peaked nature.

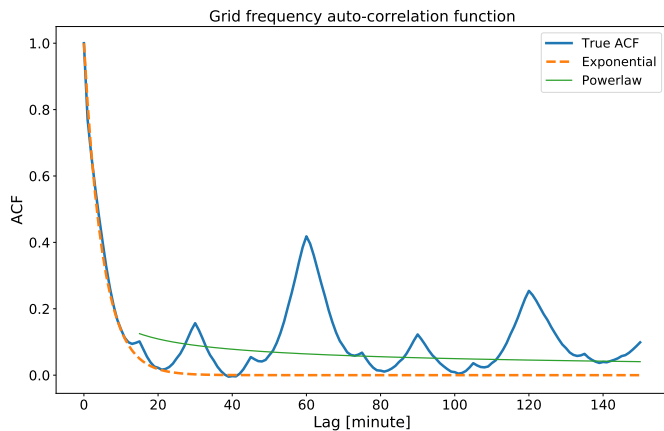


Fig. 15. European grid frequency ACF. Note the strong periodicity and power-law behaviour at longer times.

B. Nordic Grid

We show in Fig. 17 the PDF for the Nordic grid is unimodal and that despite strong correlations at longer times the ACF (Fig. 18) is well described by an exponential, suggesting ordinary Gaussian fluctuation. This is also confirmed

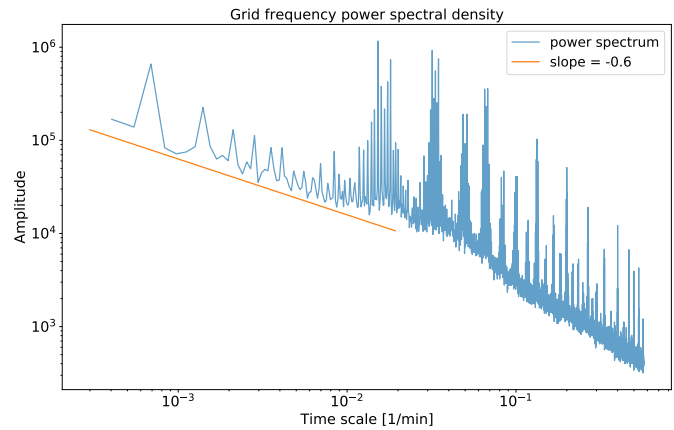


Fig. 16. European grid power spectrum. Note the non-zero slope at long time scales signalling long-term correlated noise (as opposed to simple Gaussian).

by checking the large time-scale part of the frequency power spectrum (Fig. 19). The data for the Nordic synchronous area is obtained from the Norwegian ESO [44] and consists of second by second measurements of the frequency for the year 2020.

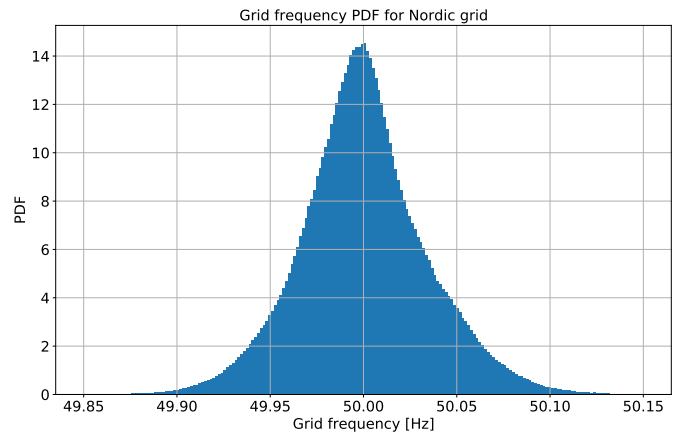


Fig. 17. Nordic grid frequency PDF. Note the uni-modal distribution.

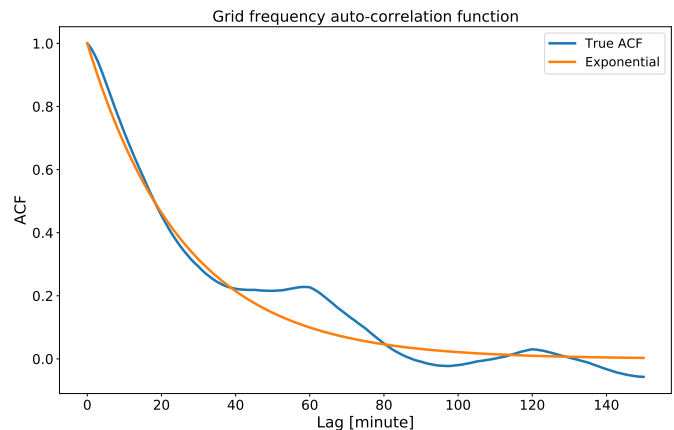


Fig. 18. Nordic grid frequency ACF. Note that despite strong correlations at about 40min the ACF is well-described by an exponential, signalling swing equation + Gaussian noise is a good description.

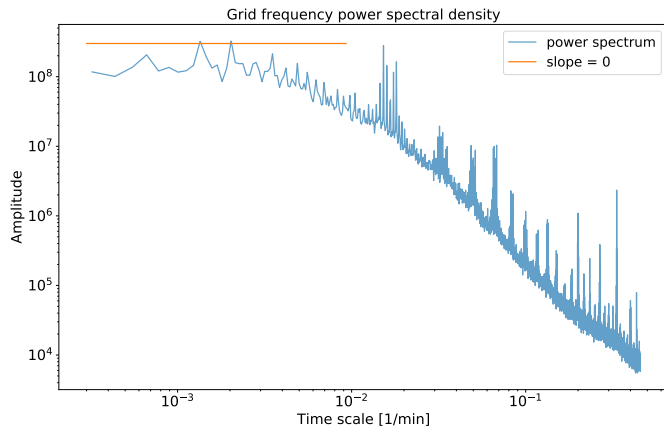


Fig. 19. Nordric grid frequency power spectrum. Note that at large time-scales the power spectrum is flat as expected for OUP (see (13)).

C. Mallorcan Grid

Mallorcan grid is a small island grid that in addition to the two peaks around the central value (as in GB, Europe) exhibits extra structure in frequency PDF (Fig. 20). Similarly as for GB and European grid we show that there are long term power-law correlations suggesting fractional noise fluctuations (Figs. 21, 22). The data was obtained from [45] and consists of 94 days of seconds-by-second measurements in 2019.

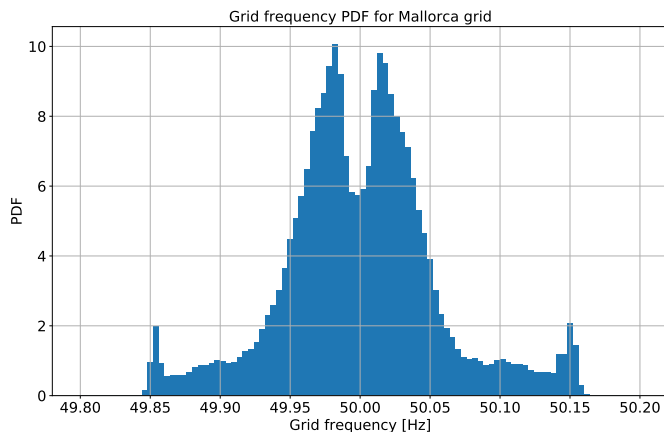


Fig. 20. Mallorcan grid frequency PDF. Note the multimodal structure suggesting additional features in the restoring term of (12), in addition to the deadband structure.

REFERENCES

- [1] S. Homan, N. Mac Dowell, and S. Brown, "Grid frequency volatility in future low inertia scenarios: Challenges and mitigation options," *Applied Energy*, vol. 290, p. 116723, 2021.
- [2] P. Tielens and D. Van Hertem, "The relevance of inertia in power systems," *Renewable and Sustainable Energy Reviews*, vol. 55, pp. 999–1009, 2016.
- [3] W. Stevenson and J. Grainger, *Power System Analysis*. McGraw-Hill Education, 1994.
- [4] F. Milano and R. Zárate-Miñano, "A systematic method to model power systems as stochastic differential algebraic equations," *IEEE Transactions on Power Systems*, vol. 28, no. 4, pp. 4537–4544, 2013.
- [5] A. J. Wood, B. F. Wollenberg, and G. B. Sheblé, *Power generation, operation, and control*. John Wiley & Sons, 2013.

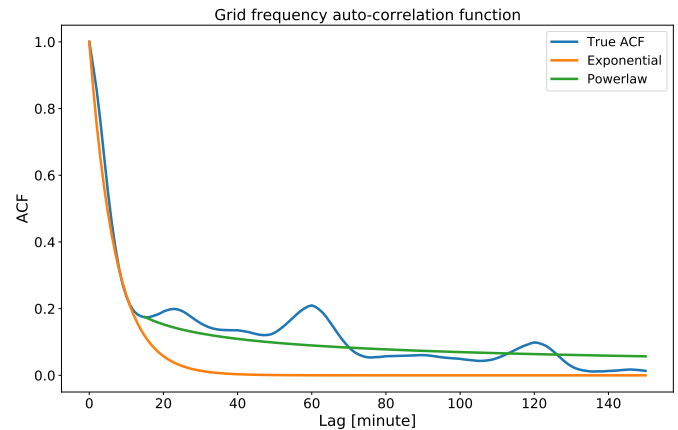


Fig. 21. Mallorcan grid frequency ACF. Note how the initial fall in correlations can be described by an exponential, but at later times it is better described by a power-law, suggesting fractional noise.

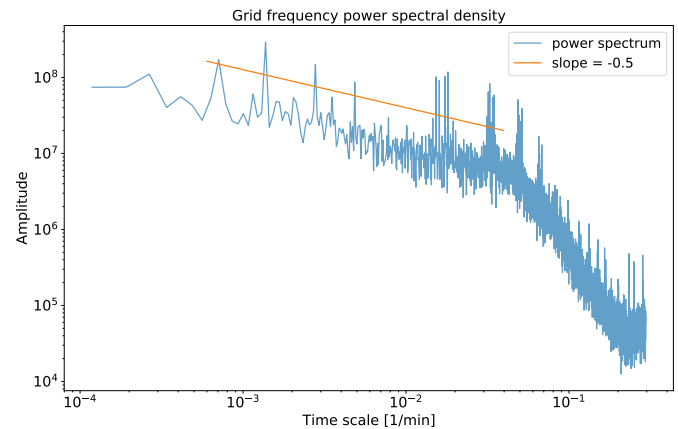


Fig. 22. Mallorcan grid frequency power spectrum. Note the non-trivial slope at large time scales suggesting fractional noise is a better description than Gaussian.

- [6] H. Zhang and P. Li, "Probabilistic analysis for optimal power flow under uncertainty," *IET Generation, Transmission & Distribution*, vol. 4, pp. 553–561(8), May 2010.
- [7] B. Schäfer, M. Matthiae, X. Zhang, M. Rohden, M. Timme, and D. Witthaut, "Escape routes, weak links, and desynchronization in fluctuation-driven networks," *Phys. Rev. E*, vol. 95, p. 060203, Jun 2017.
- [8] C. Roberts, E. M. Stewart, and F. Milano, "Validation of the ornstein-uhlenbeck process for load modeling based on μ pmu measurements," in *2016 Power Systems Computation Conference (PSCC)*, 2016, pp. 1–7.
- [9] F. M. Mele, A. Ortega, R. Zárate-Miñano, and F. Milano, "Impact of variability, uncertainty and frequency regulation on power system frequency distribution," in *2016 Power Systems Computation Conference (PSCC)*, 2016, pp. 1–8.
- [10] P. Vorobev, D. M. Greenwood, J. H. Bell, J. W. Bialek, P. C. Taylor, and K. Turitsyn, "Deadbands, droop, and inertia impact on power system frequency distribution," *IEEE Transactions on Power Systems*, vol. 34, no. 4, pp. 3098–3108, 2019.
- [11] B. Schäfer, M. Timme, and D. Witthaut, "Isolating the impact of trading on grid frequency fluctuations," in *2018 IEEE PES Innovative Smart Grid Technologies Conference Europe (ISGT-Europe)*, 2018, pp. 1–5.
- [12] L. R. Gorjão, M. Anvari, H. Kantz, C. Beck, D. Witthaut, M. Timme, and B. Schäfer, "Data-driven model of the power-grid frequency dynamics," *IEEE Access*, vol. 8, pp. 43 082–43 097, 2020.
- [13] B. Schäfer, D. Witthaut, and M. Timme, "How decentral smart grid control limits non-gaussian power grid frequency fluctuations," in *2018 IEEE Conference on Control Technology and Applications (CCTA)*, 2018, pp. 32–39.
- [14] B. Schäfer, C. Beck, K. Aihara, D. Witthaut, and M. Timme, "Non-

- Gaussian power grid frequency fluctuations characterized by Lévy-stable laws and superstatistics,” *Nature Energy*, vol. 3, p. 119, Jan 2018.
- [15] M. Anvari, L. R. Gorjão, M. Timme, D. Withaut, B. Schäfer, and H. Kantz, “Stochastic properties of the frequency dynamics in real and synthetic power grids,” *Phys. Rev. Research*, vol. 2, p. 013339, Mar 2020.
- [16] X. Deng, H. Li, W. Yu, W. Weikang, and Y. Liu, “Frequency observations and statistic analysis of worldwide main power grids using fnet/grideye,” in *2019 IEEE Power Energy Society General Meeting (PESGM)*, 2019, pp. 1–5.
- [17] D. del Giudice, A. Brambilla, S. Grillo, and F. Bizzarri, “Effects of inertia, load damping and dead-bands on frequency histograms and frequency control of power systems,” *International Journal of Electrical Power & Energy Systems*, vol. 129, p. 106842, 2021.
- [18] J. Kruse, B. Schäfer, and D. Withaut, “Predictability of power grid frequency,” *IEEE Access*, vol. 8, pp. 149 435–149 446, 2020.
- [19] A. Bolzoni, R. Todd, A. Forsyth, and R. Perini, “Real-time autoregressive modelling of electric power network frequency,” in *IECON 2019 - 45th Annual Conference of the IEEE Industrial Electronics Society*, vol. 1, 2019, pp. 515–520.
- [20] M. F. Wolff, K. Schmietendorf, P. G. Lind, O. Kamps, J. Peinke, and P. Maass, “Heterogeneities in electricity grids strongly enhance non-gaussian features of frequency fluctuations under stochastic power input,” *Chaos: An Interdisciplinary Journal of Nonlinear Science*, vol. 29, no. 10, p. 103149, 2019.
- [21] G. Filatrella, A. H. Nielsen, and N. F. Pedersen, “Analysis of a power grid using a Kuramoto-like model,” *European Physical Journal B*, vol. 61, no. 4, pp. 485–491, Feb 2008.
- [22] A. Fernández-Guillamón, E. Gómez-Lázaro, E. Muljadi, and Ángel Molina-García, “Power systems with high renewable energy sources: A review of inertia and frequency control strategies over time,” *Renewable and Sustainable Energy Reviews*, vol. 115, p. 109369, 2019.
- [23] S. C. Johnson, D. J. Papageorgiou, D. S. Mallapragada, T. A. Deetjen, J. D. Rhodes, and M. E. Webber, “Evaluating rotational inertia as a component of grid reliability with high penetrations of variable renewable energy,” *Energy*, vol. 180, pp. 258–271, 2019.
- [24] G. E. Uhlenbeck and L. S. Ornstein, “On the theory of the Brownian motion,” *Phys. Rev.*, vol. 36, pp. 823–841, Sep 1930.
- [25] O. Vasicek, “An equilibrium characterization of the term structure,” *Journal of Financial Economics*, vol. 5, no. 2, pp. 177–188, 1977.
- [26] B. Lindner, “A brief introduction to some simple stochastic processes,” *Stochastic Methods in Neuroscience*, vol. 1, 2009.
- [27] H. Fink and C. Klüppelberg, “Fractional Lévy-driven Ornstein-Uhlenbeck processes and stochastic differential equations,” *Bernoulli*, vol. 17, no. 1, pp. 484 – 506, 2011.
- [28] B. B. Mandelbrot and J. W. V. Ness, “Fractional Brownian motions, fractional noises and applications,” *SIAM Review*, vol. 10, no. 4, pp. 422–437, 1968.
- [29] J. Beran, *Statistics for long-memory processes*. CRC press, 1994, vol. 61.
- [30] P. Flandrin, “On the spectrum of fractional Brownian motions,” *IEEE Transactions on Information Theory*, vol. 35, no. 1, pp. 197–199, 1989.
- [31] J. Nolan, *Univariate Stable Distributions: Models for Heavy Tailed Data*, ser. Springer Series in Operations Research and Financial Engineering. Springer International Publishing, 2020.
- [32] T. Marquardt, “Fractional Lévy processes with an application to long memory moving average processes,” *Bernoulli*, vol. 12, no. 6, pp. 1099–1126, 2006.
- [33] S. Rostek and R. Schöbel, “A note on the use of fractional Brownian motion for financial modeling,” *Economic Modelling*, vol. 30, pp. 30–35, 2013.
- [34] D. A. Benson, M. M. Meerschaert, and J. Revielle, “Fractional calculus in hydrologic modeling: A numerical perspective,” *Advances in Water Resources*, vol. 51, pp. 479–497, 2013, 35th Year Anniversary Issue.
- [35] P. Addison and A. Ndumu, “Engineering applications of fractional Brownian motion: self-affine and self-similar random processes,” *Fractals*, vol. 7, no. 02, pp. 151–157, 1999.
- [36] “Historic frequency data for Great Britain,” Available at <https://data.nationalgrideso.com/system/system-frequency-data>.
- [37] M. Tarnopolski, “On the relationship between the Hurst exponent, the ratio of the mean square successive difference to the variance, and the number of turning points,” *Physica A: Statistical Mechanics and its Applications*, vol. 461, pp. 662–673, 2016.
- [38] F. J. Molz, H. H. Liu, and J. Szulga, “Fractional Brownian motion and fractional Gaussian noise in subsurface hydrology: A review, presentation of fundamental properties, and extensions,” *Water Resources Research*, vol. 33, no. 10, pp. 2273–2286, 1997.
- [39] S. Stoev and M. Taqqu, “Simulation methods for linear fractional stable motion and farima using the fast fourier transform,” *Fractals*, vol. 12, 01 2003.
- [40] B. M. Hill, “A Simple General Approach to Inference About the Tail of a Distribution,” *The Annals of Statistics*, vol. 3, no. 5, pp. 1163 – 1174, 1975.
- [41] P. Kloeden and E. Platen, *The Numerical Solution of Stochastic Differential Equations*, 01 2011, vol. 23.
- [42] C. R. H. et al., “Array programming with NumPy,” *Nature*, vol. 585, no. 7825, pp. 357–362, Sep. 2020.
- [43] “Historic frequency data from RTE,” Available at <https://www.services-rte.com/en/download-data-published-by-rte.html>.
- [44] “Historic frequency data from Statnett,” Available at <http://driftsdata.statnett.no/restapi/Frequency/BySecond>.
- [45] R. Jumar, H. Maaß, B. Schäfer, L. Rydin Gorjão, and V. Hagenmeyer, “Database of Power Grid Frequency Measurements,” *arXiv e-prints*, Jun. 2020.

David Kraljic received an MSci in experimental and theoretical physics from the University of Cambridge in 2012 and a DPhil in theoretical physics from the University of Oxford in 2016.

He works as a researcher in the Laboratory of Robotics, Faculty of Electrical Engineering, University of Ljubljana from 2017 focusing on gait analysis as well as industrial robotics. He also works at Comcom trading d.o.o., an electricity trading and technology company, where he focuses on power system modelling and optimisation.